

# Unmasking the Unknown: Facial Deepfake Detection in the Open-Set Paradigm

Nadarasar Bahavan, *Member, IEEE*, Sanjay Saha, *Member, IEEE*, Ken Chen, *Member, IEEE*, Sachith Seneviratne, *Member, IEEE*, Sanka Rasnayaka, *Member, IEEE*, and Saman Halgamuge, *Fellow, IEEE*

**Abstract**—Facial forgery methods such as deepfakes can be misused for identity manipulation and spreading misinformation. They have evolved alongside advancements in generative AI, leading to new and more sophisticated forgery techniques that diverge from existing “known” methods. Conventional deepfake detection methods use the closed-set paradigm, thus limiting their applicability to detecting forgeries created using methods that are not part of the training dataset. In this paper, we propose a shift from the closed-set paradigm for deepfake detection. In the open-set paradigm, models are designed not only to identify images created by known facial forgery methods but also to identify and flag those produced by previously unknown methods as “unknown” and not as un-forged/real/unmanipulated.

In this paper, we propose an open-set deepfake classification algorithm based on supervised contrastive learning. The open-set paradigm used in our model allows it to function as a more robust tool capable of handling emerging and unseen deepfake techniques, enhancing reliability and confidence, and complementing forensic analysis.

In open-set paradigm, we identify three groups including the “unknown” group that is neither considered known deepfake nor real. We investigate deepfake open-set classification across three scenarios—classifying deepfakes from unknown methods not as real, distinguishing real images from deepfakes, and classifying deepfakes from known methods—using the FaceForensics++ dataset as a benchmark. Our method achieves state of the art results in the first two tasks and competitive results in the third task.

**Index Terms**—Deepfake detection, CelebDFv2, FaceForensics++c23, Open-set Classification, Contrastive Learning

## I. INTRODUCTION

**F**ACIAL deepfake methods are deep learning-based algorithms that generate synthetic media, such as videos or images, by convincingly mimicking real people’s faces. In this context, real or unmanipulated refers to authentic, unaltered data, often described as pristine, while forged or manipulated refers to media altered through deepfake techniques. Facial deepfakes have gained widespread notoriety due to their capacity to produce strikingly realistic visual content, which can be misused by malicious entities to spread false information, manipulate identities, and infringe upon personal privacy [1], [2], [3]. The recent advancement of generative AI, coupled with increased GPU capacity and availability, has led to new techniques for creating facial deepfakes.

Most existing deepfake detectors are built on two assumptions: The testing data set is created using the same forgery techniques used to make the training data set, where both training and testing data share the same labels and feature space, and both data sets follow the same distribution. However, in real-world scenarios, it is difficult to collect training

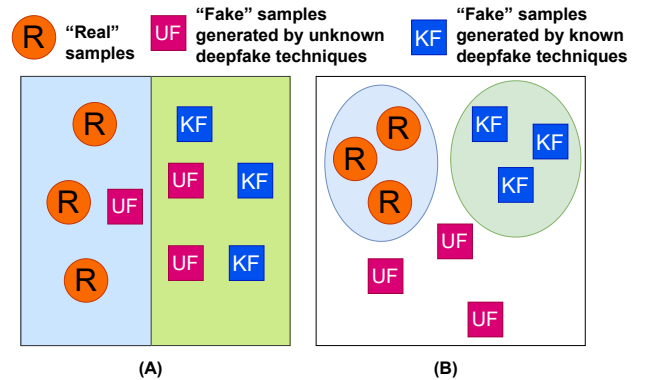


**Fig. 1:** This figure illustrates the latent space and decision boundaries of both the closed-set and open-set paradigms. (A) In the case of a closed-set classifier, the model learns a feature space and decision boundaries based solely on the known deepfake techniques and real data, distinguishing between Real and Known Deepfakes. (B) However, this approach cannot identify samples from previously unseen techniques. In contrast, open-set recognition establishes more flexible decision boundaries around the known classes and learns more general features.

data that covers all possible test categories. As a result, an image from an unknown forgery technique—a technique not encountered during training—that violates these assumptions can be incorrectly identified as real (as shown in Fig. 1 (A)). Researchers have attempted to circumvent this problem by adding various inductive biases during the model design itself based on heuristics [4], [5], [6], [7], [8], [9], [10]. However, these heuristics are derived from the observations from existing known deepfake techniques and may not apply to newer emerging techniques. Given these implications, there is an urgent need to develop a reliable deepfake detection system to detect new and emerging variants of deepfake forgery methods.

To overcome this limitation, open set recognition (OSR) offers a more practical solution, requiring the model to not only achieve high accuracy on known classes but also detect and manage samples from previously unseen categories during testing (as shown in Fig. 1 (B)). Open-set detection enables a model to recognize and appropriately handle data from classes that were not present in the training set. In the context of deepfake identification, this involves detecting not only known forgery methods but also identifying new, previously unseen forgery techniques. Rather than misclassifying these unknown forgeries as belonging to known classes, the model can flag them as unknown, thus maintaining robustness against

emerging threats [11].

This ability leads to several advantages: (A) It enhances robustness by helping models identify new deepfake methods, potentially reducing the risk of misclassification. (B) Early identification of emerging unknown forgeries enables the development of methods to prevent their future misuse by malicious actors. Forensic Experts can use few-shot or continual learning to quickly adapt models with limited data, ensuring robust detection of new deepfake techniques [12], [13].

Open-set methods operate by identifying the lack of expected features needed to classify a test sample as a known category, rather than detecting novel elements in the image, as suggested by the familiarity hypothesis [14]. This makes it crucial to develop highly discriminative features across manipulated and unmanipulated data. Supervised contrastive learning (SupCon) has proven effective for learning such discriminative features, with its success is demonstrated in open-set recognition tasks [15], [16]. However, adapting Supervised contrastive learning for deepfake detection introduces unique challenges.

In Supervised contrastive learning, deepfake forgeries often form discriminative, well-separated representations, while real data tends to have more scattered representations. This makes it challenging to distinguish real from fake data. To address this, we modify the contrastive loss to emphasize the real class, encouraging tighter clustering of real data and making its representations more compact and distinct from manipulated data. This improvement enhances the model’s ability to detect deepfakes, particularly in open-set scenarios where unknown manipulations are identified as anomalies.

We introduce a method for open-set deepfake detection designed to address situations where the model encounters unknown forgery techniques. To the best of our knowledge, this is the first work to investigate the open-set classification problem in the context of deepfakes.

We make the following contributions.

- **Representation Learning algorithm:** We propose a variant of Supervised Contrastive Learning designed specifically for deepfake problems.
- **Good performance in Unknown Deepfake Classification:** The proposed algorithm demonstrates excellent performance compared to the Xception baseline in detecting unknown deepfakes
- **Competitive Performance in Known Deepfake Classification:** In the evaluation of known deepfakes, the proposed model performs competitively with state of the art methods.
- **Good performance as a open-set detector:** In distinguishing between real and deepfake data, we demonstrate that our feature learning method effectively captures a generalizable latent space. Our approach exhibits superior open-set performance within the cross-manipulation protocol, highlighting its robustness and efficacy in handling diverse manipulation techniques.
- **Explainability through Visualization:** The use of UMAP projections [17] reveals how the model effectively distinguishes between known and unknown classes, with

unknown deepfakes clustering separately in the latent space. Furthermore, Grad-CAM visualizations [18] of real images offer interpretable insights, demonstrating the model’s focused attention on specific areas of interest. This dual approach enhances the understanding of the model’s decision-making process and its capability to identify various deepfake manipulations.

## II. RELATED WORK

### A. Facial Forgery/Deepfake Generation Methods

Deepfake generation involves three primary approaches: Identity swapping, face-reenactment, and entire image synthesis. Identity swapping swaps the identity of faces in images or videos using techniques like auto-encoder-based methods (e.g., DeepFakes [19]) and graphics-based swapping methods (e.g., FaceSwap [20]). Face-reenactment transfers facial expressions from a source video to a target video, maintaining the target person’s identity while mimicking the source’s expressions, with Face2Face [21] and Neural Textures [22] being prominent examples. Entire image synthesis generates completely new facial images without face-swapping, utilizing advanced generative models such as Generative Adversarial Networks (GANs) [23], diffusion models [24], [25], [26]. These methods enable the creation of highly realistic synthetic media, each with unique capabilities and challenges.

### B. Generalizable Deepfake detectors

Deepfake detection faces significant challenges with generalization. Most of them are designed with a closed-set classifier. Current efforts are divided into image forgery and video forgery detection. In the realm of image forgery, innovative solutions have emerged, including frequency clues [27], [28], [29], [30], designed networks [31], [32], disentanglement learning [33], [34], [35], reconstruction learning [36], [37], data augmentation [38], [39] and 3D decomposition [40]. Conversely, recent works in video forgery detection focus on optical flow [41], eye blinking [42], neuron behaviors [43], and temporal inconsistencies [44], [45].

### C. Open-set deepfake detection.

As per the writer’s knowledge the only work done in open-set recognition for facial forgery detection is done by Xu et al. [46]. The key limitation is that the method is it relies on the shared characteristics of the training datasets to detect new forgeries and mistakenly makes the closed-set assumption. It also uses a feature fusion of multiple neural networks for representation learning and doesn’t investigate open-set detection algorithms.

### D. Representation Learning

Metric learning is a machine learning technique that represents images as points in a special space called “latent space”. In this space, each image is turned into a point, or “embedding”. The key idea is that the closer two points are in this space, the more similar their corresponding images are. If

two images look alike, their points will be close together, and if they are different, their points will be farther apart.

Using various methods such as contrastive learning and supervised contrastive learning, we can define the important characteristics that the model should focus on. This allows the model to better understand and compare images based on these specific features.

In contrastive learning, we teach a model to recognize similarities and differences between images by creating “similar” images through slight changes to the original, like rotating or cropping it [47]. These altered versions are treated as similar, while entirely different images are treated as dissimilar. This helps the model learn that certain objects remain similar even after transformations like rotation.

In supervised contrastive learning, labels are used to guide the model in understanding which images are similar and which are different [48]. Images that belong to the same category (or class) are given embeddings (points in the latent space) that are close to each other, while images from different categories are assigned embeddings that are farther apart. This approach helps the model learn to group similar images and separate different ones based on their labels.

### III. METHODS

Each deepfake image forgery is unique, depending on the generation method used, such as GANs or autoencoders. The main goal of the method is to design a latent space that captures only the forgery-specific characteristics of an image, ignoring irrelevant details such as identity, background, or lighting. By focusing solely on the forgery traits, the model avoids learning features that may be common across both real and manipulated data, thus improving its ability to distinguish forgeries from real images. This is achieved using weighted supervised contrastive learning, where forged images are assigned labels based on their specific forgery characteristics. The weighting ensures that the model prioritizes these forgery-specific features, leading to more cohesive and accurate representations. This approach helps the representation learning model to focus solely on distinguishing the most discriminative features relevant to deepfake detection.

Once a latent space is constructed using weighted supervised contrastive learning in Stage 01, decision boundaries are established in Stage 02. These boundaries help address the open-set problem, where the model identifies unknown test classes that were not seen during training. In Stage 03, thresholds are determined based on confidence scores, allowing the model to detect whether a test sample belongs to one of the known classes or is an unknown class. This process is visualized as a three-stage pipeline in Fig 2.

#### A. Preliminaries/Supervised Contrastive Learning

Let  $\{\mathbf{x}_k, \mathbf{y}_k\}_{k=1}^N$  represent  $N$  labeled samples from a given batch of training image data with  $C$  classes. From the given training batch, we create an augmented training batch of  $2N$  samples (multi-viewed batch), represented as  $\{\tilde{\mathbf{x}}_\ell, \tilde{\mathbf{y}}_\ell\}_{\ell=1}^{2N}$ .

In this multi-viewed batch,  $\tilde{\mathbf{x}}_{2k-1}$  and  $\tilde{\mathbf{x}}_{2k}$  are two random augmentations of  $\mathbf{x}_k$  for each  $k = 1, \dots, N$ . These augmentations could include changes like rotations, flips, or color

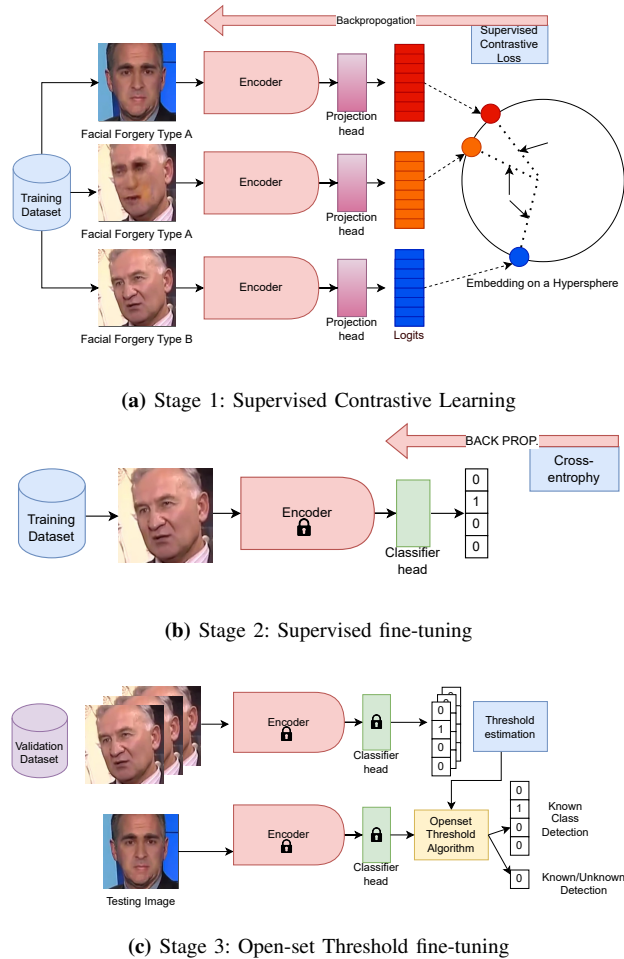


**Fig. 2:** This figure shows the proposed methodology. (a) Supervised contrastive learning is used on the dataset to learn representations of various deepfake/real images via an encoder. (b) During the second stage, the encoder is frozen and a classifier is learnt on top of it. (c) In this phase, the logits of the training samples are employed to establish thresholds, which are then utilized for detecting unknown classes.

adjustments which preserve a subset of the original image’s information. Both of these new images share the same label as the original image, meaning  $\tilde{\mathbf{y}}_{2k-1} = \tilde{\mathbf{y}}_{2k} = \mathbf{y}_k$

In addition to rotations, flips, or color adjustment, it implicitly treats different identities, poses, and lighting as augmentations of a particular type of specific deepfake.

The multi-viewed batch of images is first propagated through an encoder network, denoted as  $Enc(\cdot)$ , to obtain a 128-dimensional embedding  $\mathbf{r}_i = Enc(\mathbf{x}_i) \in \mathcal{R}^{128}$ . Subsequently, this embedding is processed through a projection network consisting of a linear layer, producing a vector  $\mathbf{z}_i = Proj(\mathbf{r}_i) \in \mathcal{R}^{128}$  as illustrated in Fig.2. The supervised contrastive loss (1) at the outputs of the projection network is used to train the model.

During our experiments, DenseNets gave the best results for the encoder choice [49].

$$\mathcal{L}_{out}^{sup}(\tau, I, y) = \sum_{i \in I} \frac{-1}{|P(i)|} \sum_{p \in P(i)} \log \left( \frac{\exp(z_i \cdot z_p / \tau)}{\sum_{a \in A(i)} \exp(z_i \cdot z_a / \tau)} \right) \quad (1)$$

**Given:**

- $I$  is the set of all samples in the batch.
- The index  $i$  is the anchor.
- $A(i)$  is the all the samples in the batch excluding the anchor.
- $y_i$  is the label for sample  $i$ .
- The set of positive samples for sample  $i$ , denoted as  $P(i)$ , is:

$$P(i) = \{p \mid y_p = y_i\}$$

This means that for every sample  $p$  in the dataset, it belongs to  $P(i)$  if its label  $y_p$  matches the label of sample  $i$ , i.e.,  $y_p = y_i$ .

- $\tau \in \mathcal{R}^+$  is a scalar temperature parameter

### B. Stage 1: Weighted Supervised Contrastive Learning

In the context of supervised contrastive learning, the real data class poses unique challenges as it often fails to form compact representations in the feature space. To address this, we modify the supervised contrastive loss to emphasize the real class, encouraging tighter clustering of real data samples.

$$\mathcal{L}_{out}^{sup}(\tau, I, y) = \sum_{i \in I} \frac{-s(i, p)}{\sum_{a \in A(i)} s(i, a)} \sum_{p \in P(i)} W(i, p, A(i)) \quad (2)$$

$$W(z_i, z_p, A(i)) = \log \left( \frac{\exp(z_i \cdot z_p / \tau)}{\sum_{a \in A(i)} \exp(z_i \cdot z_a / \tau)} \right) \quad (3)$$

To further guide the representation learning, a pairwise similarity scaling factor  $s(i, j)$  is introduced to prioritize certain relationships between samples based on their manipulation status:

$$s(i, j) = \begin{cases} \alpha & \text{if } i \text{ and } j \text{ are both real,} \\ 0 & \text{if } i \text{ and } j \text{ are not equal to each other} \\ 1 & \text{otherwise.} \end{cases} \quad (4)$$

The contrastive loss is designed to place greater emphasis on clustering real data samples tightly in the feature space. By assigning higher weights  $s(i, j)$  to pairs of real data, the model learns more cohesive representations of real samples.

### C. Stage 2: Supervised fine-tuning

For improved generalization and overall performance, the Stochastic Moving Average (SWA) encoder  $\tilde{Enc}(\cdot)$  is constructed by averaging multiple trained encoder weights [50].

Next, the input batch undergoes processing through the SWA encoder network  $\tilde{Enc}(\cdot)$  to obtain embeddings. These embeddings are then fed into a classifier network  $f(\cdot)$  and trained using cross-entropy loss [51]. The classifier network predicts outputs  $\hat{y} = f(\mathbf{r}) \in \mathcal{R}^{D_P}$ .

### D. Stage 3: The Open-Set Detection Algorithm

In the third stage, the classifier  $f(\cdot)$  learns to predict the probability of an input belonging to a specific class. This probability is denoted as  $\hat{y}_i$ , calculated by:

$$y_i = P(y_i = 1 \mid x) = \frac{e^{f_i(\tilde{Enc}(x))}}{\sum_{j=1}^K e^{f_j(\tilde{Enc}(x))}} \quad (5)$$

Here,  $f_i(\cdot)$  represents the classifier's output for class  $i$ , and  $y_i$  indicates whether the input's label belongs to class  $i$ .

The open-set algorithm determines rejection thresholds using a method called thresholding on the training dataset, detailed in Algorithm 1. This algorithm calculates thresholds for each class to determine whether a sample belongs to the class or should be rejected as unknown. It works by gathering confidence scores (softmax probabilities) of correctly classified training samples, then setting a threshold based on a specified percentile of these scores.

The process of open-set detection is explained in Algorithm 2. This algorithm checks if a test sample belongs to any known class or should be flagged as unknown. It compares the sample's confidence score for each class against the precomputed thresholds; if none are met, the sample is labeled as unknown.

This approach is advantageous because it does not require additional samples from new classes for fine-tuning, unlike traditional open-set detection methods.

---

#### Algorithm 1 Estimation of Class-wise Rejection Thresholds

---

- 1: Initialize empty set  $T_i$  for each class  $i$
  - 2: **for** each training example  $(x, y)$  **do**
  - 3:     Calculate the softmax probabilities  $\hat{y}_i$  using Eq.5
  - 4:     Find the predicted class  $i = \arg \max_i P(y_i = 1 \mid x)$
  - 5:     **if**  $y = i$  **then**
  - 6:         Add the output logit  $\hat{y}_i$  to the set  $T_i$
  - 7:     **end if**
  - 8: **end for**
  - 9: **for** each class  $i$  **do**
  - 10:     Sort the set  $T_i$
  - 11:     Calculate the  $\lambda$  percentile of  $T_i$  and record it as  $\epsilon_i$
  - 12: **end for**
- 

---

#### Algorithm 2 Open-set classification

---

- 1: **for** each test sample  $x$  **do**
  - 2:     Find the predicted logits  $P(y_i = 1 \mid x)$  for all classes
  - 3:     Set  $is\_unknown \leftarrow True$
  - 4:     **for** each class  $i$  **do**
  - 5:         **if**  $P(y_i = 1 \mid x) \geq \epsilon_i$  **then**
  - 6:              $is\_unknown \leftarrow False$
  - 7:         **break**
  - 8:     **end if**
  - 9:     **end for**
  - 10:     **if**  $is\_unknown$  **then**
  - 11:         Label  $x$  as an unknown sample
  - 12:     **end if**
  - 13: **end for**
-

#### IV. EXPERIMENTAL EVALUATION

This section details the data processing pipeline and evaluation strategies employed for both the Cross-manipulation and Cross-dataset evaluations, as presented in the results section.

##### A. Datasets

The cross-manipulation evaluation utilizes the FaceForensics++23 (FF++c23) dataset [52]. FF++c23 consists of 1,000 pristine videos, each featuring a unique individual in a distinct background. Additionally, it includes 4,000 forged videos derived from these pristine videos, generated using four different face manipulation algorithms, as illustrated in Fig 3: Face2Face (F2F) [21], DeepFakes (DF) [19], NeuralTextures (NT) [22], and FaceSwap (FS) [20]. DF (DeepFakes) and FS (FaceSwap) are identity-swapping methods, which involve replacing the identity of a person in a video or image with that of another individual. In contrast, NT (NeuralTextures) and F2F (Face2Face) are facial reenactment methods, which manipulate the expressions or motions of a subject’s face while preserving their original identity.

The cross-dataset evaluation incorporates both the FaceForensics++23 dataset and the CelebDF dataset [53].

##### B. Baseline Model

Due to the novelty of our method, some results are compared against a baseline model. This baseline employs an Xception architecture and follows the exact training methodology outlined in [52].

##### C. Cross-manipulation Evaluation

In real-world detection scenarios, defenders often lack detailed knowledge of the specific forgery techniques employed by attackers. Therefore, it is essential to evaluate the model’s ability to recognize unfamiliar forgery methods as unknown. This assessment is particularly important in cross-manipulation settings, where the model encounters a variety of forgery techniques that were not present during training. Our approach aligns with the methodology proposed by Xu et al. [46].

The dataset has a total of five classes: the pristine videos and its four manipulated versions. For each class, its videos are split into three sets according to the protocol of Xu et al. [46]: 600 for training, 200 for validation and 200 for testing. Each pristine video and its respective four manipulated versions are kept together in the same set.

Each video consists of a series of images called frames. Given that the algorithm processes images, we select 10 random frames from each video instead of using the entire video. We use multitask cascaded computational neural networks (MTCNN) [54] to crop the face from the background. Afterwards, the cropped images were resized to a size of  $224 \times 224$  pixels.

Open-set classification aims to differentiate between known classes, which the model has been trained on, and unknown classes, which it has not encountered before. For our dataset,



**Fig. 3:** Sample face images from different facial forgery methods utilized in this study. The first column showcases pristine (non-manipulated) frames, while the subsequent four columns depict images generated by DeepFakes (DF), Face2Face (F2F), FaceSwap (FS), and Neural Textures (NT). DF and FS are identity swapping methods whereas NT and F2F are Facial Re-enactment methods

FF++c23 which has 5 classes, we evaluated four distinct combinations of known and unknown classes. Each combination is made by reserving one of the four facial forgery methods as unknown.

For each combination, the model is trained on the train sets of the known classes and then tested on the test sets of the unknown and known classes. The performance metrics were then documented for each combination.

##### D. Cross-Dataset Evaluation

During the cross-dataset evaluation, the model is trained on all classes from the FF++c23 dataset. In this phase, the real class from the CelebDFv2 dataset is treated as the known “real” class, while the fake class is designated as the “unknown” class. This evaluation follows the same image processing methodology as the cross-manipulation evaluation.

##### E. Metrics

We report the results as AUROC (Area Under the Receiver Operating Characteristic curve) and True Open-Set Classification (TOSC) Accuracy.

**True-Open-Set-Classification (TOSC) Accuracy / Open Set Classification Rate.** This accounts for the unknown samples:

$$\text{TOSC} = \frac{\sum_{i=1}^{C+1} (TP_i + TN_i)}{\sum_{i=1}^{C+1} (TP_i + TN_i + FP_i + FN_i)} \quad (6)$$

$TN_i$ ,  $TP_i$ ,  $FN_i$ ,  $FP_i$  represent the True Negative, True Positive, False Negative, False Positive for a class  $i$ . The known classes are denoted by  $\{1, 2, \dots, C\}$ .  $C + 1$  is the unknown test class.

**Area Under Receiver Operating Curve (AUROC).** To calculate the AUROC for open-set unknown classes, we evaluate how well a model can distinguish known classes (positive) from unknown classes (negative). This process requires adapting the traditional AUROC computation to the context of open set recognition. The AUROC for unknown classes is calculated following the methodology outlined in a recent survey [55].

**TABLE I:** Unknown class detection using the frame-level AUROC metric. The row is a model trained on the training classes and then tested on a test dataset containing an unknown class. The proposed model significantly outperforms the Xception baseline in all the instances. Higher values of AUROC are optimal

Unknown Testing Class	Training Classes	Proposed	Xception
DF	F2F,FS,NT	<b>0.7189</b>	0.5184
F2F	DF,FS,NT	<b>0.7399</b>	0.5458
FS	DF,F2F,NT	<b>0.5672</b>	0.4671
NT	DF,F2F,FS	<b>0.8233</b>	0.5985

**TABLE II:** Unknown class detection using the frame-level AUROC metric. The row is a model trained on the training classes and then tested on a test dataset containing an unknown class. Here the The proposed model significantly outperforms the Xception baseline in all the instances. Higher values of AUROC are optimal

Unknown Testing Class	Type of Test Class	Training Classes	Type of Training Classes	Proposed	Xception
FS	Identity Swapping	F2F,NT	Face reenactment	<b>0.4904</b>	0.4781
DF	Identity Swapping	F2F,NT	Face reenactment	<b>0.8023</b>	0.5125
NT	Face reenactment	DF,FS	Identity Swapping	<b>0.7264</b>	0.5671
F2F	Face reenactment	DF,FS	Identity Swapping	<b>0.7410</b>	0.5475

## V. RESULTS

We examine deepfake classification across three open-set scenarios using the cross-manipulation evaluation described in Section IV-C: (A) detecting unknown deepfakes, (B) detecting known deepfakes, and (C) detecting deepfakes. The differences between these three cases are highlighted in Fig 1. The benchmark dataset used for comparison in this section is the widely recognized FaceForensics++c23 (FF++c23) dataset, which serves as the gold standard for deepfake detection research [46].

Subsequently, we focus on the explainability of our method, conducting additional experiments to assess cross-dataset performance using both the FaceForensics++c23 and CelebDFv2 datasets [52], [53].

### A. Open-set classification of Unknown deepfakes

For each combination of training and testing classes based on FF++c23 (described in Section IV-C), we measure the Area Under the ROC Curve (AUROC) for detecting the unknown test class, as shown in Table I.

Our experimental results consistently demonstrate high AUROC values, indicating strong model performance in detecting unknown deepfake techniques. Furthermore, our method significantly outperforms the Xception baseline (detailed in Section IV-B) across various training and testing class combinations. These findings highlight the robustness of our approach in open-set detection scenarios. For example, in Table I, when the unknown testing class is DF, the proposed model achieves an AUROC of 0.7189, compared to Xception’s 0.5184, representing a substantial improvement of over 20 percentage points. Similarly, for the NT unknown testing class, the proposed model attains an AUROC of 0.8233, significantly surpassing Xception’s 0.5985.

In Table II, we further evaluate the method’s performance in open-set scenarios where the unknown class belongs to a different type of deepfake method. These results confirm the robustness of our approach in detecting previously unseen types of deepfakes. For instance, in Table I, when the unknown testing class is DF—an identity-swapping method—and the

training data contains face reenactment methods, the proposed model achieves an AUROC of 0.8023, compared to Xception’s 0.5125, marking a significant improvement of over 30 percentage points. Similarly, for the NT unknown testing class—a face reenactment method—the proposed model achieves an AUROC of 0.7264, vastly outperforming Xception’s 0.5671.

### B. Open-Set Classification of Known Deepfakes

To evaluate our system, we analyze its ability to identify unseen test samples of known forgeries. This evaluation method, widely adopted in the literature, often emphasizes specialization over generalization.

The results presented in Table III show the evaluation of our proposed method on the FaceForensics++ dataset (FF++c23) across different manipulation types: DeepFake (DF), Face2Face (F2F), FaceSwap (FS), and NeuralTextures (NT). Our method demonstrates competitive results and performs comparably across various manipulations, particularly on FaceSwap (FS), where it achieves 0.9943 AUROC. For NeuralTextures (NT), the proposed method shows slightly lower performance (0.9512 to 0.9307) but remains competitive compared to other approaches. Our method is an open-set classifier whereas the others are closed-set classifiers. Despite this, our model still achieved competitive results, suggesting that the learned features are generalizable across manipulations.

### C. Open-set classification of deepfakes

This focuses on detecting any deepfake (known or unknown) as a singular category. The TOSC (True Open-Set Classification from Section IV-E) metric was employed, but instead of rejecting unknown instances as “unknown”, the model classified both known and unknown deepfakes as “deepfake”. This modification consolidates the task into detecting manipulation, regardless of whether it is known or unknown. It follows the protocol described in [46].

As seen in Table IV, the proposed one-class model achieves state-of-the-art (SOTA) performance across several unknown classes. Compared to the baseline results reported in [46], our model consistently outperforms other methods. Notably, the

**TABLE III:** This table shows the evaluation of known deepfakes with frame level AUROC % metric for our method. We compare it with closed-set detectors referenced in [56], but the results are not strictly comparable due to the open-set nature of our method. For each method, the model’s performance (Frame Level AUROC%) is estimated on an equal split of the corresponding deepfake method and real data. Higher values are optimal

Methodology	Backbone	Type of Model	Training Data	Testing Classes			
				DF	F2F	FS	NT
MIL [57]	Xception	Closed-set	FF++c23	99.51	98.59	94.86	97.96
XN-avg [58]	Xception	Closed-set	FF++c23	99.38	99.53	99.36	97.29
Face X-ray [59]	HRNet	Closed-set	FF++c23	99.12	99.31	99.09	99.27
S-MIL-T [60]	Xception	Closed-set	FF++c23	99.84	99.34	99.61	98.85
PCL + I2G [56]	Xception	Closed-set	FF++c23	100.00	99.57	100.00	99.58
Proposed	DenseNet121	Open-set	FF++c23, DF excluded	-	97.87	99.43	93.07
Proposed	DenseNet121	Open-set	FF++c23, F2F excluded	98.63	-	98.47	93.00
Proposed	DenseNet121	Open-set	FF++c23, FS excluded	99.15	98.64	-	95.1
Proposed	DenseNet121	Open-set	FF++c23, NT excluded	98.96	97.02	97.60	-
Proposed	DenseNet121	Open-set	FF++c23	98.96	99.2	99.42	96.14

**TABLE IV:** TOSC Accuracy obtained on the unknown classes from various state-of-the-art approaches against proposed approaches in the cross-manipulation testing regime. Higher values are optimal. Results are taken directly from [46]. The best results are highlighted in bold and the second is underlined. (N.R means that the original paper has not reported the corresponding result.)

Methodology	Unknown Class			
	DF	F2F	FS	NT
CLRNet [61]	50.12	53.73	50.00	69.75
TAR [62]	75.25	72.90	51.65	N.R
DDT [63]	78.82	N.R	N.R	64.10
Xception [64]*	82.73	64.69	49.74	55.59
Fusion [46]	<b>83.99</b>	64.69	49.77	55.59
Proposed	<u>83.95</u>	<b>79.77</b>	<b>76.12</b>	<b>81.22</b>

proposed approach demonstrates superior accuracy in detecting both known and unknown deepfakes, achieving 83.95% on the DF class and a substantial improvement across the other classes, with 79.77% on F2F, 76.12% on FS, and 81.22% on NT. This places our model ahead of all compared methodologies in every scenario, delivering significant advancements in deepfake detection accuracy.

*D. Explainability*

The proposed method detects unknown samples by thresholding the model’s softmax outputs, rejecting samples with low output scores. In essence, this approach identifies unknowns by recognizing the absence of features required to classify a test sample into any known class, rather than detecting novel features within the image.

This means that when the model identifies a known facial forgery, it focuses on a single, strong discriminative feature. On the other hand, when the model encounters an unknown facial forgery, it relies on a broader set of weaker features. By visualizing the class activation maps, we can observe this behavior [18]. For known facial forgeries, the class activations are more concentrated, whereas for unknown facial forgeries, the activations are more diffuse and spread out.

*E. Cross-dataset performance and evaluation.*

Most existing research has relied on the FF++c23 dataset, which serves as a suitable benchmark. However, it is crucial

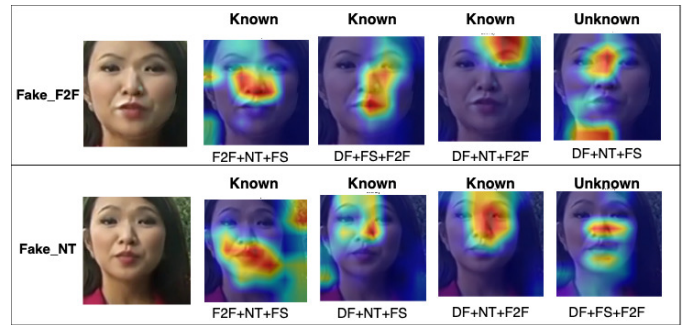


**Fig. 4:** Class activation maps produced for images created by known and unknown facial forgeries for two different cases of unknown test classes. Notably, the images with unknown facial forgeries show multiple clusters of activations.

to evaluate models against other datasets for rigorous benchmarking. A key challenge in cross-dataset evaluation is the domain shift, particularly concerning real images. Real images from different datasets (such as FF++c23, CelebDF, or StarGAN) may vary in terms of lighting, resolution, compression artifacts, and even subject demographics. These differences can result in models trained on FF++c23 generalizing poorly when tested on other datasets, especially for real image classification. Furthermore, many datasets include a mixture of forgery methods, which introduces a blend of known and unknown manipulation techniques, making it difficult to track and evaluate the model’s performance across these varying methods.

These two implications mean it is difficult to evaluate the model’s capacity as an unknown deepfake /known deepfake detector for datasets aside from FF++c23. Thus we investigate its performance as a “general deepfake detector”.

The results as shown in Table V indicate, according to the CelebDF dataset, our method remains competitive [53], outperforming methods such as Meso4 [65], FAW [39], Face X-ray [38].

**TABLE V:** Cross-dataset evaluations using the frame-level AUROC metric on the deepfake benchmark [66]. All detectors are trained on FF++c23 [52] and evaluated on other datasets.

Detector	CDF-v2
Meso4 [65]	0.609
MesoIncep [65]	0.697
CNN-Aug [67]	0.703
Xception [52]	0.737
EfficientB4 [68]	0.749
CapsuleNet [69]	0.747
FWA [39]	0.668
Face X-ray [38]	0.679
FFD [31]	0.744
CORE [70]	0.743
Recce [37]	0.732
UCF [34]	0.753
F3Net [27]	0.735
SPSL [29]	0.765
SRM [28]	0.755
Proposed	0.695

## VI. ABLATION STUDIES

### A. Impact of Pairwise similarity scaling factor in Stage 1

We modified the supervised contrastive loss to focus on improving the clustering of real data samples, which often fail to form compact representations in the feature space as introduced in Section III-B. By introducing a pairwise similarity scaling factor, we prioritize real data pairs, encouraging tighter clustering and enhancing the representation learning of real samples. The alpha parameter controls the influence of the real data samples in the loss function. In this section, we explore the effects of various values of the alpha parameter on the overall performance.

When alpha is 0, the algorithm becomes the conventional supervised contrastive learning. Table VI illustrates the effect of the alpha factor. As observed, as alpha increases from zero, we get improvements in the performance: however it degrades for larger values of alpha. This is potentially due to an overemphasis on real data pairs, which may reduce the model’s ability to capture the underlying differences between manipulated samples, leading to less effective generalization. Therefore, careful tuning of the alpha parameter is essential to balance the influence of real data samples and manipulation-related variations.

**TABLE VI:** Unknown class detection evaluated using frame-level AUROC for varying alpha values. The best results are highlighted in bold.

Unknown Class	1	1.21	2.25	4
DF	0.7009	<b>0.7189</b>	0.7119	0.7076
F2F	0.7129	<b>0.7399</b>	0.7219	0.7126
FS	0.6113	<b>0.6781</b>	0.6610	0.6580
NT	0.7877	<b>0.8233</b>	0.8100	0.7926

### B. Impact of Labeling Scheme in Stage 1

Table VII compares the impact of two labeling schemes on model performance during Stage 01 training:

- **Scheme 1:** Samples are labeled based on the specific forgery method used (e.g., FaceSwap (FS), DeepFake (DF), Face2Face (F2F), and NeuralTextures (NT)).

- **Scheme 2:** Samples are labeled only as real or fake.

As shown in Table VII, using a fine grained, forgery-specific labeling scheme (Scheme 1) significantly improves the model’s ability to detect unknown forgeries. This improvement arises because Scheme 1 enables the model to learn highly discriminative, method-specific features unique to each forgery technique, with minimal overlap between features of different methods. In contrast, Scheme 2 captures only general discriminative features shared across all forgery methods, which limits its ability to generalize effectively. The granularity of Scheme 1’s feature representation equips the model to better recognize distinctive manipulation patterns, enhancing its ability to classify previously unseen forgery methods as unknown.

**TABLE VII:** Unknown class detection evaluated using frame-level AUROC. Each row represents a model trained on known classes and tested on unknowns. Scheme 1 uses forgery-specific labels, while Scheme 2 indicates whether an image is fake or real. The best results are highlighted in bold.

Unknown Class	Scheme 1	Scheme 2
DF	<b>0.7189</b>	0.5841
F2F	<b>0.7399</b>	0.6784
FS	<b>0.6781</b>	0.5672
NT	<b>0.8233</b>	0.5432

### C. Impact of Representation Learning Method in Stage 1

Several representation learning methods have been proposed in the literature. Cross-entropy (CE) remains the most widely used approach [71]. Recently, supervised contrastive learning (SupCon) has emerged as a more effective method for learning highly discriminative features, as demonstrated by its superior AUROC for unknown class detection and the well-structured organization of its latent space [72]. Additionally, SIMCLR is a widely recognized unsupervised feature learning technique [47].

The impact of these representation learning methods on detecting unknown classes is summarized in Table VIII, where SupCon is shown to outperform the other approaches.

Comparing the discriminative features learned by SupCon and CE is crucial for understanding their relative effectiveness. t-SNE visualizations illustrate that SupCon achieves superior separation of unknown features from real class features, demonstrating greater intra-class compactness and inter-class separation. The t-SNE plots for each method are shown in Fig. 5a, and Fig. 5b, with the unknown class NT and manipulated images highlighted in yellow. A major challenge for the encoder is avoiding the misclassification of unknown classes as unmanipulated (real). SupCon effectively addresses this issue, as evidenced in Fig. 5a ( In the figure, there is less mixing of the green(real) and yellow (unknown) points.), where unknown classes are clearly distinguished from both real and manipulated classes compared to cross entropy (Fig. 5b). This robustness in feature learning underscores the documented strengths of supervised contrastive learning [48].



**TABLE VIII:** Unknown class detection using the frame-level AUROC metric. Each column represents an unknown class, and each row shows the model’s AUROC performance on that class. Higher AUROC values are optimal.

Representation Learning Method	Unknown Class			
	DF	F2F	FS	NT
SupCon	0.7009	0.7129	0.611	0.7877
Cross Entropy	0.6787	0.5888	0.5564	0.6313
SIMCLR	0.5012	0.5045	0.5034	0.4998
<b>Proposed</b>	<b>0.7189</b>	<b>0.7399</b>	<b>0.678</b>	<b>0.8233</b>

*D. Impact of Labelling Schema in Stage 3*

Open-set detection is a rapidly evolving field. Many existing approaches, such as OpenMax [11] and Membership Loss [73], depend on additional unknown data for model fine-tuning. In contrast, softmax thresholding delivers robust performance while maintaining results comparable to closed-set classifiers for known classes.

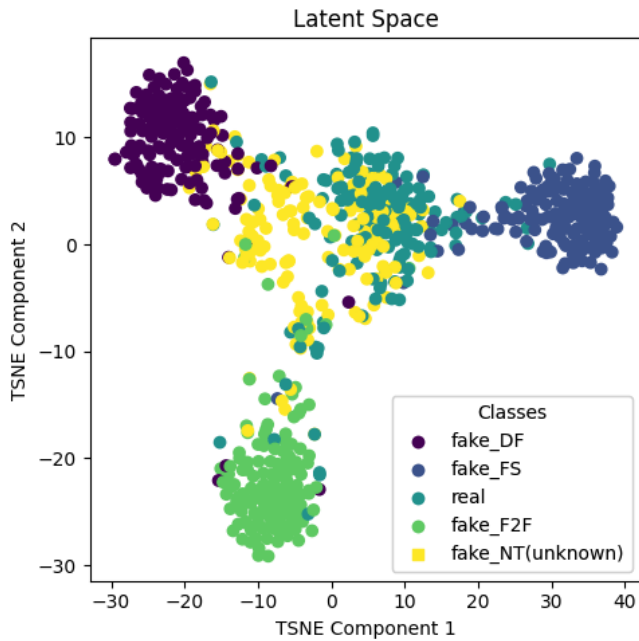
Table IX compares the impact of two labeling schemes on model performance during Stage 02 training:

- **Scheme 1:** Samples are labeled based on the specific forgery method used (e.g., FaceSwap (FS), DeepFake (DF), Face2Face (F2F), and NeuralTextures (NT)).
- **Scheme 2:** Samples are labeled only as real or fake.

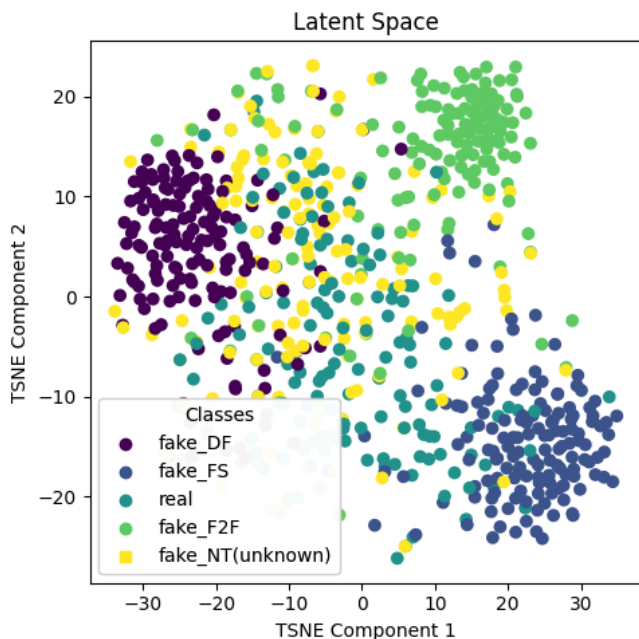
As observed in Table IX, giving fine-grained forgery specific information leads to better performance in unknown class detection.

**TABLE IX:** Unknown class detection using the frame-level AUROC metric. The row is a model trained on the training classes and then tested on the unknown class. Scheme 1 refers to forgery specific labels. Scheme 2 identifies if the image is real or fake. Higher values of AUROC are optimal

Unknown Class	Scheme 1	Scheme 2
DF	<b>0.7189</b>	0.6841
F2F	<b>0.7399</b>	0.6784
FS	<b>0.5672</b>	0.511
NT	<b>0.8233</b>	0.7432



(a) Weighted Supervised Contrastive Learning



(b) Cross Entropy

**Fig. 5:** This figure shows the TSNE visualizations of the representations learned by various methods

VII. CONCLUSION AND FUTURE WORK

We propose an open-set deepfake detection framework based on supervised contrastive learning. Experiments using the publicly available FaceForensics++23 dataset demonstrate the effectiveness of our approach, achieving comparable or superior performance on detecting images forged by known and unknown deepfake techniques.

Future work can address the following limitations: As shown by cross-dataset evaluations, the current method is sensitive to discrepancies between the real training and testing data distributions, particularly when the real data experiences domain shifts. Adopting a video level approach, incorporating more localized priors for facial features, could theoretically alleviate these issues observed during cross-dataset testing and should be explored in future research.

ACKNOWLEDGMENT

NB acknowledges Melbourne Graduate Research Scholarship. The authors would like to thank Yu Xia, Jayanie Bogahawatte and Chathura Jayasankha for proof-reading the document. This research was supported by The University of Melbourne’s Research Computing Services .

REFERENCES

[1] Department of Homeland Security, “Increasing threat of deepfake identities,” Department of Homeland Security, Tech. Rep., 2023. [Online]. Available: [https://www.dhs.gov/sites/default/files/publications/increasing\\_threats\\_of\\_deepfake\\_identities\\_0.pdf](https://www.dhs.gov/sites/default/files/publications/increasing_threats_of_deepfake_identities_0.pdf)

- [2] KPMG, “Deepfakes: Real threat,” KPMG International, Tech. Rep., 2023. [Online]. Available: <https://kpmg.com/kpmg-us/content/dam/kpmg/pdf/2023/deepfakes-real-threat.pdf>
- [3] Trend Micro. (2022) How underground groups use stolen identities and deepfakes. [Online]. Available: [https://www.trendmicro.com/en\\_au/research/22/i/how-underground-groups-use-stolen-identities-and-deepfakes.html](https://www.trendmicro.com/en_au/research/22/i/how-underground-groups-use-stolen-identities-and-deepfakes.html)
- [4] B. Zhou, A. Khosla, A. Lapedriza, A. Oliva, and A. Torralba, “Learning deep features for discriminative localization,” in *Proceedings of the IEEE Conference on Computer Vision and Pattern Recognition (CVPR)*, 2016, pp. 2921–2929.
- [5] H. Zhao, W. Zhou, D. Chen, T. Wei, W. Zhang, and N. Yu, “Multi-attentional deepfake detection,” in *Proceedings of the IEEE/CVF Conference on Computer Vision and Pattern Recognition (CVPR)*, June 2021, pp. 2185–2194.
- [6] X. Yang, Y. Li, and S. Lyu, “Exposing deep fakes using inconsistent head poses,” in *Proceedings of the IEEE International Conference on Acoustics, Speech and Signal Processing (ICASSP)*, 2019, pp. 8261–8265.
- [7] E. Sabir, J. Cheng, A. Jaiswal, W. AbdAlmageed, I. Masi, and P. Natarajan, “Recurrent convolutional strategies for face manipulation detection in videos,” in *Proceedings of the IEEE/CVF Conference on Computer Vision and Pattern Recognition Workshops*, 2019.
- [8] A. Rössler, D. Cozzolino, L. Verdoliva, C. Riess, J. Thies, and M. Nießner, “Faceforensics++: Learning to detect manipulated facial images,” in *Proceedings of the IEEE/CVF International Conference on Computer Vision*, 2019.
- [9] Y. Qian, G. Yin, L. Sheng, Z. Chen, and J. Shao, “Thinking in frequency: Face forgery detection by mining frequency-aware clues,” in *Proceedings of the European Conference on Computer Vision*, 2020.
- [10] Y. Li and S. Lyu, “Exposing deepfake videos by detecting face warping artifacts,” in *Proceedings of the IEEE/CVF Conference on Computer Vision and Pattern Recognition Workshops*, 2019.
- [11] A. Bendale and T. E. Boult, “Towards open set deep networks,” in *Proceedings of the IEEE Conference on Computer Vision and Pattern Recognition*, 2016, pp. 1563–1572.
- [12] L. Guan, F. Liu, R. Zhang, J. Liu, and Y. Tang, “Mcv: A generalizable deepfake detection method for few-shot learning,” *Sensors*, vol. 23, no. 21, p. 8763, 2023.
- [13] Anonymous, “Towards generalized deepfake detection with continual learning on limited new data,” *ResearchGate*, 2023, publication details not fully available.
- [14] T. G. Dietterich and A. Guyer, “The familiarity hypothesis: Explaining the behavior of deep open set methods,” *Pattern Recogn.*, vol. 132, no. C, Dec. 2022. [Online]. Available: <https://doi.org/10.1016/j.patcog.2022.108931>
- [15] Y. Kodama, Y. Wang, R. Kawakami, and T. Naemura, “Open-set recognition with supervised contrastive learning,” in *2021 17th International Conference on Machine Vision and Applications (MVA)*, 2021, pp. 1–5.
- [16] B. Xu, F. Shen, and J. Zhao, “Contrastive open set recognition,” in *Proceedings of the AAAI Conference on Artificial Intelligence*, vol. 37, no. 9, 2023, pp. 10 546–10 556.
- [17] L. McInnes, J. Healy, and J. Melville, “Umap: Uniform manifold approximation and projection for dimension reduction,” *arXiv preprint arXiv:1802.03426*, 2018.
- [18] R. R. Selvaraju, M. Cogswell, A. Das, R. Vedantam, D. Parikh, and D. Batra, “Grad-cam: Visual explanations from deep networks via gradient-based localization,” in *Proceedings of the IEEE International Conference on Computer Vision*, 2017, pp. 618–626.
- [19] DeepFakes, “Faceswap,” <https://github.com/deepfakes/faceswap>, 2020, accessed: 2020-09-02.
- [20] M. Kowalski, “Faceswap,” <https://github.com/MarekKowalski/FaceSwap>, 2021, accessed: 2020-09-03.
- [21] J. Thies, M. Zollhöfer, M. Stamminger, C. Theobalt, and M. Nießner, “Face2face: Real-time face capture and reenactment of rgb videos,” in *Proceedings of the IEEE Conference on Computer Vision and Pattern Recognition (CVPR)*, 2016, pp. 2387–2395.
- [22] J. Thies, M. Zollhöfer, and M. Nießner, “Deferred neural rendering: Image synthesis using neural textures,” *ACM Transactions on Graphics*, vol. 38, no. 4, pp. 1–12, 2019.
- [23] I. J. Goodfellow, J. Pouget-Abadie, M. Mirza, B. Xu, D. Warde-Farley, S. Ozair, A. Courville, and Y. Bengio, “Generative adversarial nets,” in *Advances in Neural Information Processing Systems*, 2014.
- [24] Y. Choi, M. Choi, M. Kim, J.-W. Ha, S. Kim, and J. Choo, “Stargan: Unified generative adversarial networks for multi-domain image-to-image translation,” in *Proceedings of the IEEE Conference on Computer Vision and Pattern Recognition*, 2018, pp. 8789–8797.
- [25] T. Karras, S. Laine, and T. Aila, “A style-based generator architecture for generative adversarial networks,” in *Proceedings of the IEEE/CVF Conference on Computer Vision and Pattern Recognition (CVPR)*, 2019, pp. 4401–4410.
- [26] J. Ho, A. Jain, and P. Abbeel, “Denoising diffusion probabilistic models,” in *Advances in Neural Information Processing Systems*, vol. 33, 2020, pp. 6840–6851.
- [27] Y. Qian, G. Yin, L. Sheng, Z. Chen, and J. Shao, “Thinking in frequency: Face forgery detection by mining frequency-aware clues,” in *European Conference on Computer Vision*. Springer, 2020, pp. 86–103.
- [28] Y. Luo, Y. Zhang, J. Yan, and W. Liu, “Generalizing face forgery detection with high-frequency features,” in *Proceedings of the IEEE/CVF Conference on Computer Vision and Pattern Recognition (CVPR)*, 2021, pp. 16 317–16 326.
- [29] H. Liu, X. Li, W. Zhou, Y. Chen, Y. He, H. Xue, W. Zhang, and N. Yu, “Spatial-phase shallow learning: Rethinking face forgery detection in frequency domain,” in *Proceedings of the IEEE/CVF Conference on Computer Vision and Pattern Recognition (CVPR)*, 2021, pp. 772–781.
- [30] Q. Gu, S. Chen, T. Yao, S. Chen, W. Ding, and L. Li, “Exploiting fine-grained face forgery clues via progressive enhancement learning,” *arXiv preprint arXiv:2112.13977*, 2021.
- [31] H. Dang, F. Liu, J. Stehouwer, X. Liu, and A. K. Jain, “On the detection of digital face manipulation,” in *Proceedings of the IEEE/CVF Conference on Computer Vision and Pattern Recognition*, 2020, pp. 5781–5790.
- [32] H. Zhao, W. Zhou, D. Chen, T. Wei, W. Zhang, and N. Yu, “Multi-attentional deepfake detection,” in *Proceedings of the IEEE/CVF Conference on Computer Vision and Pattern Recognition (CVPR)*, June 2021, pp. 2185–2194.
- [33] X. Liang, H. Shi, and W. Deng, “Exploring disentangled content information for face forgery detection,” in *European Conference on Computer Vision*. Springer, 2022, pp. 128–145.
- [34] Z. Yan, Y. Zhang, Y. Fan, and B. Wu, “Ucf: Uncovering common features for generalizable deepfake detection,” in *Proceedings of the IEEE/CVF International Conference on Computer Vision*, 2023, pp. 22 412–22 423.
- [35] T. Yang, J. Cao, Q. Sheng, L. Li, J. Ji, X. Li, and S. Tang, “Learning to disentangle gan fingerprint for fake image attribution,” *arXiv preprint arXiv:2106.08749*, 2021.
- [36] C. Wang and W. Deng, “Representative forgery mining for fake face detection,” in *Proceedings of the IEEE/CVF Conference on Computer Vision and Pattern Recognition (CVPR)*, 2021, pp. 14 923–14 932.
- [37] J. Cao, C. Ma, T. Yao, S. Chen, S. Ding, and X. Yang, “End-to-end reconstruction-classification learning for face forgery detection,” in *Proceedings of the IEEE/CVF Conference on Computer Vision and Pattern Recognition*, 2022, pp. 4113–4122.
- [38] L. Li, J. Bao, T. Zhang, H. Yang, D. Chen, F. Wen, and B. Guo, “Face x-ray for more general face forgery detection,” in *Proceedings of the IEEE/CVF Conference on Computer Vision and Pattern Recognition*, 2020, pp. 5001–5010.
- [39] Y. Li and S. Lyu, “Exposing deepfake videos by detecting face warping artifacts,” *arXiv preprint arXiv:1811.00656*, 2018.
- [40] X. Zhu, H. Wang, H. Fei, Z. Lei, and S. Z. Li, “Face forgery detection by 3d decomposition,” in *Proceedings of the IEEE/CVF Conference on Computer Vision and Pattern Recognition (CVPR)*, June 2021, pp. 2929–2939.
- [41] I. Amerini, L. Galteri, R. Caldelli, and A. Del Bimbo, “Deepfake video detection through optical flow based cnn,” in *Proceedings of the IEEE/CVF International Conference on Computer Vision (ICCV) Workshops*, October 2019, pp. 1205–1207.
- [42] Y. Li, M.-C. Chang, and S. Lyu, “In ictu oculi: Exposing ai created fake videos by detecting eye blinking,” in *Proceedings of the IEEE International Workshop on Information Forensics and Security (WIFS)*, 2018, pp. 1–7.
- [43] R. Wang, F. Juefei-Xu, L. Ma, X. Xie, Y. Huang, J. Wang, and Y. Liu, “Fakespotter: A simple yet robust baseline for spotting ai-synthesized fake faces,” *arXiv preprint arXiv:1909.06122*, 2019.
- [44] A. Haliassos, K. Vougioukas, S. Petridis, and M. Pantic, “Lips don’t lie: A generalisable and robust approach to face forgery detection,” in *Proceedings of the IEEE/CVF Conference on Computer Vision and Pattern Recognition (CVPR)*, June 2021, pp. 5039–5049.
- [45] C. Wang, J. Bao, W. Zhou, W. Wang, and H. Li, “Altfreezing for more general video face forgery detection,” in *Proceedings of the IEEE/CVF Conference on Computer Vision and Pattern Recognition (CVPR)*, June 2023, pp. 4129–4138.
- [46] Y. Xu, K. Raja, and M. Pedersen, “Supervised contrastive learning for generalizable and explainable deepfakes detection,” in *Proceedings of*

- the *IEEE/CVF Winter Conference on Applications of Computer Vision*, 2022, pp. 379–389.
- [47] T. Chen, S. Kornblith, M. Norouzi, and G. Hinton, “A simple framework for contrastive learning of visual representations,” in *Proceedings of the 37th International Conference on Machine Learning*, ser. Proceedings of Machine Learning Research, vol. 119. PMLR, 2020, pp. 1597–1607.
- [48] P. Khosla, P. Teterwak, C. Wang, A. Sarna, Y. Tian, P. Isola, A. Maschinot, C. Liu, and D. Krishnan, “Supervised contrastive learning,” in *Proceedings of the 34th International Conference on Neural Information Processing Systems*, ser. NIPS’20. Red Hook, NY, USA: Curran Associates Inc., 2020.
- [49] G. Huang, Z. Liu, L. van der Maaten, and K. Q. Weinberger, “Densely connected convolutional networks,” in *Proceedings of the IEEE Conference on Computer Vision and Pattern Recognition*, 2017.
- [50] G. Yang, T. Zhang, P. Kirichenko, J. Bai, A. G. Wilson, and C. De Sa, “Swalp: Stochastic weight averaging in low-precision training,” *arXiv preprint arXiv:1904.11943*, 2019.
- [51] Y. Zhong and M. Mohri, “Cross-entropy loss functions: Theoretical analysis and applications,” *arXiv preprint arXiv:2304.07288*, 2023.
- [52] A. Rössler, D. Cozzolino, L. Verdoliva, C. Riess, J. Thies, and M. Nießner, “Faceforensics++: Learning to detect manipulated facial images,” in *Proceedings of the IEEE/CVF International Conference on Computer Vision*, 2019, pp. 1–11.
- [53] Y. Li, X. Yang, P. Sun, H. Qi, and S. Lyu, “Celeb-df: A large-scale challenging dataset for deepfake forensics,” in *IEEE Conference on Computer Vision and Pattern Recognition (CVPR)*, 2020.
- [54] K. Zhang, Z. Zhang, Z. Li, and Y. Qiao, “Joint face detection and alignment using multitask cascaded convolutional networks,” in *IEEE Signal Processing Letters*, vol. 23, no. 10. IEEE, 2016, pp. 1499–1503.
- [55] C. Geng, S. jun Huang, and S. Chen, “Recent advances in open set recognition: A survey,” *IEEE Transactions on Pattern Analysis and Machine Intelligence*, vol. 42, no. 7, pp. 1619–1636, 2020.
- [56] T. Zhao, X. Xu, M. Xu, H. Ding, Y. Xiong, and W. Xia, “Learning self-consistency for deepfake detection,” in *2021 IEEE/CVF International Conference on Computer Vision (ICCV)*, 2021, pp. 15 003–15 013.
- [57] X. Wang, Y. Yan, P. Tang, X. Bai, and W. Liu, “Revisiting multiple instance neural networks,” *Pattern Recognition*, vol. 74, pp. 15–24, 2018.
- [58] A. Rössler, D. Cozzolino, L. Verdoliva, C. Riess, J. Thies, and M. Nießner, “Faceforensics++: Learning to detect manipulated facial images,” in *Proceedings of the IEEE/CVF International Conference on Computer Vision*, Oct. 27–Nov. 2 2019, pp. 1–11.
- [59] L. Li, J. Bao, T. Zhang, H. Yang, D. Chen, F. Wen, and B. Guo, “Face x-ray for more general face forgery detection,” in *Proceedings of the IEEE/CVF Conference on Computer Vision and Pattern Recognition*, Jun. 14–19 2020, pp. 5001–5010.
- [60] X. Li, Y. Lang, Y. Chen, X. Mao, Y. He, S. Wang, H. Xue, and Q. Lu, “Sharp multiple instance learning for deepfake video detection,” in *Proceedings of the 28th ACM International Conference on Multimedia*. ACM, Oct. 12–16 2020.
- [61] S. Tariq, S. Lee, H. Kim, Y. Shin, and S. S. Woo, “A convolutional lstm based residual network for deepfake video detection,” *arXiv preprint arXiv:2009.07480*, 2020.
- [62] —, “Tar: Generalized forensic framework to detect deepfakes using weakly supervised learning,” in *IFIP International Conference on ICT Systems Security and Privacy Protection*. Springer, 2021, pp. 387–401.
- [63] S. Aneja and M. Nießner, “Generalized zero and few-shot transfer for facial forgery detection,” *arXiv preprint arXiv:2006.11863*, 2020.
- [64] F. Chollet, “Xception: Deep learning with depthwise separable convolutions,” in *Proceedings of the IEEE Conference on Computer Vision and Pattern Recognition*, 2017, pp. 1800–1807.
- [65] D. Afchar, V. Nozick, J. Yamagishi, and I. Echizen, “Mesonet: a compact facial video forgery detection network,” in *2018 IEEE International Workshop on Information Forensics and Security*. IEEE, 2018, pp. 1–7.
- [66] Z. Yan, Y. Zhang, X. Yuan, S. Lyu, and B. Wu, “Deepfakebench: A comprehensive benchmark of deepfake detection,” *arXiv preprint arXiv:2307.01426*, 2023.
- [67] K. He, X. Zhang, S. Ren, and J. Sun, “Deep residual learning for image recognition,” in *Proceedings of the IEEE/CVF Conference on Computer Vision and Pattern Recognition*, 2016, pp. 770–778.
- [68] M. Tan and Q. Le, “Efficientnet: Rethinking model scaling for convolutional neural networks,” in *International Conference on Machine Learning*. PMLR, 2019, pp. 6105–6114.
- [69] H. H. Nguyen, J. Yamagishi, and I. Echizen, “Capsule-forensics: Using capsule networks to detect forged images and videos,” in *IEEE International Conference on Acoustics, Speech and Signal Processing*. IEEE, 2019, pp. 2307–2311.
- [70] Y. Ni, D. Meng, C. Yu, C. Quan, D. Ren, and Y. Zhao, “Core: Consistent representation learning for face forgery detection,” in *Proceedings of the IEEE/CVF Conference on Computer Vision and Pattern Recognition Workshop*, 2022, pp. 12–21.
- [71] A. Mao, M. Mohri, and Y. Zhong, “Cross-entropy loss functions: Theoretical analysis and applications,” *arXiv preprint arXiv:2304.07288*, 2023. [Online]. Available: <https://arxiv.org/abs/2304.07288>
- [72] P. Khosla, P. Teterwak, C. Wang, A. Sarna, Y. Tian, P. Isola, A. Maschinot, C. Liu, and D. Krishnan, “Supervised contrastive learning,” in *Advances in Neural Information Processing Systems*, H. Larochelle, M. Ranzato, R. Hadsell, M. Balcan, and H. Lin, Eds., vol. 33. Curran Associates, Inc., 2020, pp. 18 661–18 673.
- [73] P. Perera and V. M. Patel, “Deep transfer learning for multiple class novelty detection,” in *Proceedings of the IEEE/CVF Conference on Computer Vision and Pattern Recognition*, 2019, pp. 11 544–11 552.



**Nadarasar Bahavan** is a Ph.D. candidate in the School of Electrical, Mechanical and Infrastructure Engineering at the University of Melbourne. His research focuses on Openset detection. He received the B.Sc. degree (Hons.) in Biomedical Engineering from the Engineering Faculty, University of Moratuwa, Sri Lanka, in 2022.



**Sanjay Saha** is a Ph.D. candidate in Computer Science at the National University of Singapore (NUS) and currently works as a Machine Learning Engineer at TikTok Pte Ltd. His research focuses on biometric data forensics, particularly face image synthesis, deepfakes, and detection of synthesized content. He holds a Bachelor’s and a Master’s degree in Computer Science from the University of Dhaka in Bangladesh.



**Ken Chen** is a PhD candidate in the School of Electrical, Mechanical and Infrastructure Engineering, University of Melbourne. He obtained his Bachelor’s and Master’s degrees from Zhejiang University, China. His research focuses on large foundation models, multi-modal learning, and responsible AI.



**Sachith Seneviratne** received the B.Sc. degree in computer science and engineering from the University of Moratuwa, Sri Lanka, and the Ph.D. degree in AI from Monash University, Australia. He is a Research Fellow at The University of Melbourne. His current research interests include deep learning, with a focus on contrastive representation learning and applications. He is broadly interested in self-supervised deep learning approaches across various disciplines, such as computer vision, graph neural networks and tabular data.



tication.

**Sanka Rasnayaka** received the B.Sc. degree (Hons.) in computer science and engineering from the Engineering Faculty, University of Moratuwa, Sri Lanka, in 2016, and the Ph.D. degree in computer science from the School of Computing, National University of Singapore, for his work on continuous authentication for mobile devices, in 2021. He is currently a Lecturer with the School of Computing, National University of Singapore. His research interests include applications of AI and computer vision. He mainly works in the fields of biometrics and authentication.



**Saman Halgamuge** (Fellow, IEEE) received the BSc engineering degree in electronics and telecommunication from the University of Moratuwa, Sri Lanka, and the Dipl.-Ing and PhD degrees in data engineering from the Technical University of Darmstadt, Germany. He is currently a professor with the Department of Mechanical Engineering, School of Electrical Mechanical and Infrastructure Engineering, University of Melbourne. He is listed as a top 2searcher for AI and Image Processing in the Stanford database. He was a distinguished lecturer of IEEE Computational Intelligence Society (2018-21). He supervised 50 PhD students and 16 postdocs in Australia to completion. His research is funded by Australian Research Council, National Health and Medical Research Council, US DoD Biomedical Research program and International industry. His previous leadership roles include head, School of Engineering, Australian National University and associate dean of the Engineering and IT Faculty, University of Melbourne